Heteromeric completive self-sorting in coordination cage systems

Elie Benchimol‡, Irene Regeni‡, Bo Zhang, Michele Kabiri, Julian J. Holstein and Guido H. Clever*

Department of Chemistry and Chemical Biology, TU Dortmund University, Otto-Hahn Str. 6, 44227 Dortmund, Germany

Self-assembly, self-sorting, coordination cages, systems chemistry.

ABSTRACT: Heteroleptic coordination cages, non-statistically assembled from a set of matching ligands, can be obtained by mixing individual components or via cage-to-cage transformations from homoleptic precursors. Based on the latter approach, we here describe a new level of self-sorting in coordination cage systems, namely 'heteromeric completive self-sorting'. Here, two heteroleptic assemblies of type $Pd_2A_2B_2$ and $Pd_2A_2C_2$, sharing one common ligand component A but differing in the other, are shown to co-exist in solution. This level of self-sorting can either be reached from a statistical mixture of assemblies based on some ligands B and C, or, alternatively, following a first step of integrative self-sorting giving a distinct $Pd_2B_2C_2$ intermediate. While subtle enthalpic factors dictate the outcome of the self-sorting, we found that it is controllable. From a unique set of three ligands, we demonstrate the transition from strict integrative self-sorting forming a Pd_2AB_2C cage to heteromeric completive self-sorting to give $Pd_2A_2B_2$ and $Pd_2A_2C_2$ by variation of the ligand ratio. Cage-to-cage transformations were followed by NMR and MS experiments. Single crystal X-ray structures for three new heteroleptic cages were obtained, impressively highlighting the versatility of ligand A to either form a π-stacked *trans*-figure-of-eight arrangement in $Pd_2A_2B_2$, or occupy two *cis*-edges in $Pd_2A_2C_2$ or only a single edge in Pd_2AB_2C. This study paves the way towards the control of heteroleptic cage populations in a systems chemistry context with emerging features such as chemical information processing, adaptive guest selectivity or stimuli-responsive catalytic action.

Introduction

Self-sorting refers to the peculiar phenomenon that mixtures, containing several different molecules recognizing and associating with each other, produce a defined assembly rather than a collection of all possible combinations of components. Such organized systems possess a higher information content[1,2] in comparison to statistical mixtures. Self-sorting is a crucial phenomenon in biology, enabling the formation of complex structures through the selective association of different subcomponents. This phenomenon is also an important factor in the field of 'systems chemistry', in particular when competing association events lead to adaptive populations of assemblies, cross-talk between co-existing species and various emergent properties.[3–8] With the aim of pushing the level of control over multicomponent systems, supramolecular chemists set their focus on strategies for the exclusive formation of discrete self-sorted structures, composed of a defined set of building blocks. Achieving this so-called 'integrative self-sorting' has proven to be a real challenge, as both enthalpic and entropic factors must be considered to overcome narcissistic sorting or the formation of statistical mixtures.[4]

Recently, we and others have developed multiple strategies to control the selective formation of discrete heteroleptic metal-organic structures through integrative self-sorting.[9] Among these, shape-complementary assembly (SCA),[10–16] coordination-sphere engineering (CSE),[17–20] ligand-ligand interactions[21,22] or guest templation[23–26] are the most commonly used. Recently we have reported an unprecedented Pd_2ABCD C_s-symmetrical assembly[27] where four different bis-monodentate ligands can fuse into a unique discrete cage under thermodynamic control, thus maximizing the structural complexity of such a fourfold-bridged dinuclear cage. Others have recently realized dinuclear Pd(II) assemblies composed of three different ligands, either in the crystalline state[28] or in solution,[29] as well as systems assembled from four different ligands under kinetic control[30] or by taking advantage of an ancillary pairing approach.[31]

While the majority of previous studies on artificial heteroleptic assembly were aimed at producing a single discrete species in solution, biological systems are composed of a multitude of co-existing complex assemblies that either act together or perform separate functions. This requires multiple non-covalent assemblies to operate under the same set of conditions and in an orthogonal fashion. Mimicking such a level of complexity has proven to be one of the most difficult tasks in supramolecular chemistry, in particular in dynamic equilibria.[22,32–37]

Here, we present what is, to the best of our knowledge, the first example of the cage-to-cage transformation of three homoleptic metallosupramolecular assemblies to a defined mixture of two co-existing heteroleptic coordination cages (Figure 1). Moreover, while both heteroleptic assemblies share one ligand (ligand **A** in Figure 1; based on a diketopyrrolopyrrole[38]), this component shows a pronouncedly different behaviour in the co-existing assemblies. This type of self-sorting was described by Schmittel and co-workers as "heteromeric completive self-sorting"[39] and is similar to a fusion of the effects of both integrative and narcissistic self-sorting. While all the components of the system are capable of forming homoleptic assemblies as well as heteroleptic $Pd_2A_2B_2$ cages by integrative self-sorting, the 1:1 mixture of co-existing heteroleptic species constitutes the thermodynamic sink of the system. We shed light on the subtle parameters allowing this self-sorting to take place by showing that small geometrical differences between ligands lead to considerable changes. Finally, we demonstrate control over strict integrative and heteromeric completive self-sorting in a three components system *via* variation of the respective ratio of its components.[40] As this represents the first example of co-existence of heteroleptic assemblies in a controlled manner, it paves the way to controlling populations of multi-functional cages with application potential in systems chemistry.

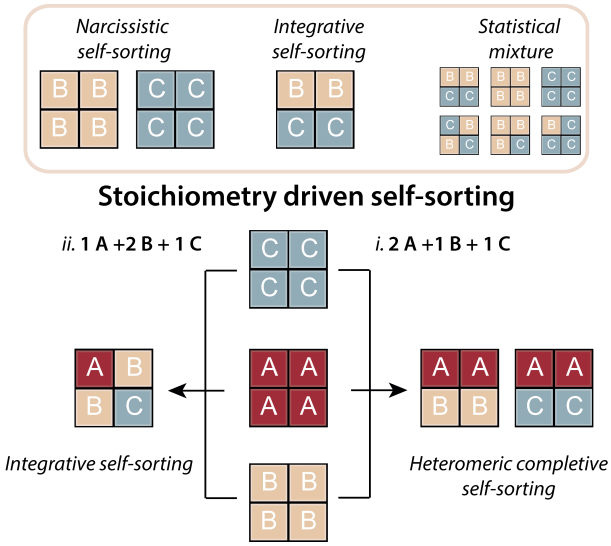

Figure 1. Step-by-step heteromeric self-sorting leading to two heteroleptic assemblies co-existing in a 1:1 ratio.

Results and Discussion

We previously reported the synthesis of ligands **A** and **B1**-**3**, all forming homoleptic assemblies when reacted with a Pd(II) source (see Figure S1 for a complete list of ligands). Ligands **B1**-**3** afford classical lantern shape Pd_2L_4 cages,[18,41,42] while **A**, bearing quinoline donor groups, forms an interlaced $Pd_2\mathbf{A}_3(MeCN)_2$ (named $Pd_2\mathbf{A}_3\mathbf{S}_2$ in the figures) ravel with one coordination site per Pd(II) cation occupied by a solvent molecule due to geometrical constraints (represented by an A_4 assembly in the more general schemes in Figures 1 and 4).[38] When mixing $Pd_2(\mathbf{B1})_4$ and $Pd_2(\mathbf{B2})_4$, we obtained a statistical mixture of assemblies $Pd_2(\mathbf{B1})_n(\mathbf{B2})_{4-n}$ (n = 0…4).[27] This is not surprising, as both ligands' binding vectors are nearly identical due to the geometrical resemblance between the backbones. Both ligands **B1** and **B2** yield a figure-of-eight *trans*-heteroleptic assembly when associated with **A** and Pd(II) in acetonitrile.[38] ESI-MS analysis confirmed the formation of a compound of stoichiometry $Pd_2(\mathbf{A})_2(\mathbf{B2})_2$ and the ^{1}H-NMR data indicated the formation of a self-penetrating structure (Figures S2-8 and S50 for model). When the homoleptic assembly $Pd_2\mathbf{A}_3(MeCN)_2$ was added to a solution containing the statistical mixture of Pd(II)-mediated assemblies from **B1** and **B2** we first obtained a very complex ^{1}H-NMR spectrum (Figure S35). However, ESI-MS analysis allowed us to decipher the outcome of the reaction, showing that $Pd_2\mathbf{A}_2(\mathbf{B1})_2$, $Pd_2(\mathbf{B1})\mathbf{A}_2(\mathbf{B2})$ and $Pd_2\mathbf{A}_2(\mathbf{B2})_2$ form as a *pseudo*-statistical mixture (Figure 2a; Figure S36). The complexity of the NMR spectrum can therefore be explained by the presence of three different heteroleptic assemblies. From this mixture, we obtained red crystalline plates suitable for X-ray diffraction analysis and unveiling the structure of $Pd_2(\mathbf{B1})\mathbf{A}_2(\mathbf{B2})$ (Figure 2b). This is the first architecture presenting a ternary *trans*-Pd_2AB_2C figure-of-eight topology, where both ligands **A** adopt an *S*-shape conformation and **B1** and **B2** complete the square-planar coordination sphere of the Pd(II) cations in a *trans*-arrangement. Owing to the strong structural similarity between **B1** and **B2**, a second level of integrative self-sorting does not proceed here, therefore leading to a statistical arrangement of the two outer ligand alternatives around the central pair of ligands **A**.

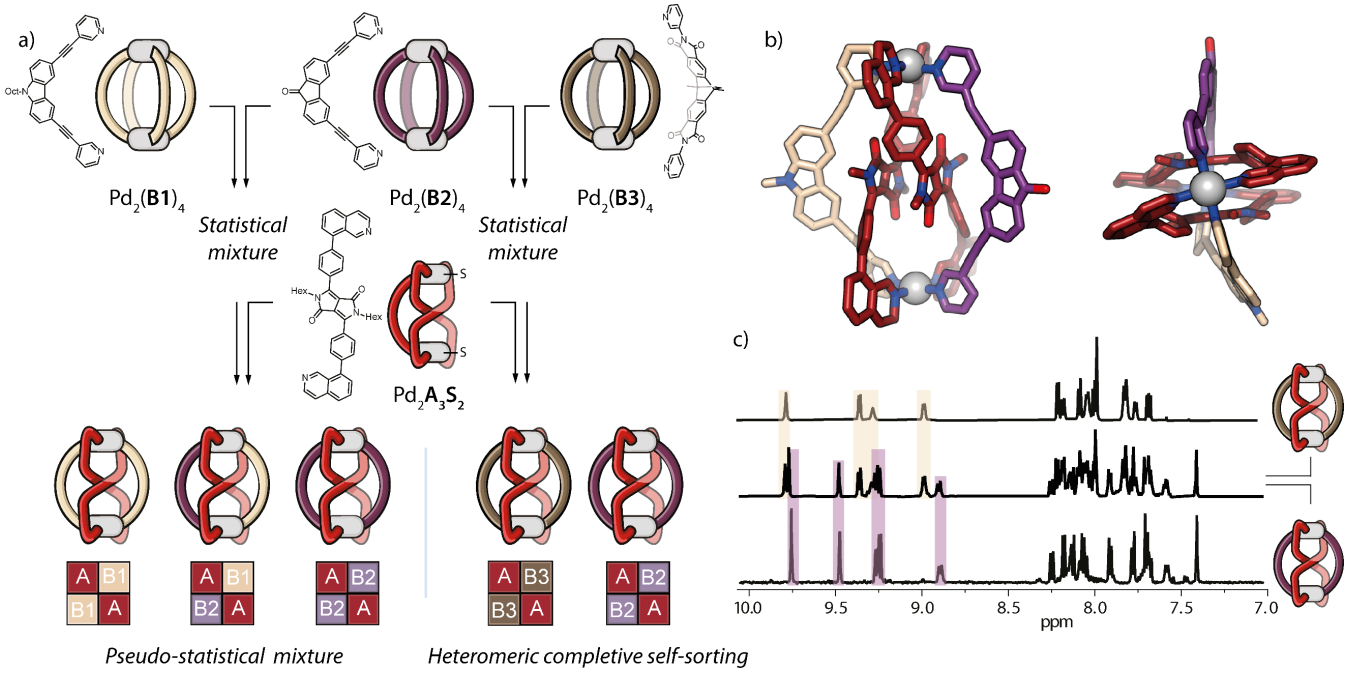

Figure 2. (a) Schematic representation of the two types of self-sorting phenomena obtained from initially statistical mixtures. In the case of **B1** and **B2**, the addition of **A** leads to a pseudo-statistical mixture. However, for **B2** and **B3** the heteromeric completive self-sorted state can be reached selectively. S = solvent molecules, herein acetonitrile. (b) Crystal structure of $Pd_2(\mathbf{B1})\mathbf{A}_2(\mathbf{B2})_2$ with a *trans*-Pd_2BA_2C figure-of-eight topology. This product was obtained selectively through crystallization. Octyl chains on the beige carbazole ligand are omitted for clarity. (c) ^{1}H-NMR (CD_3CN, 500 MHz) stack of the two-separate figure-of-eight structures $Pd_2\mathbf{A}_2(\mathbf{B2})_2$ and $Pd_2\mathbf{A}_2(\mathbf{B3})_2$ and the heteromeric completive self-sorting result after mixing.

In contrast, when ligand **B3** (Figure 2a) was utilized, we were indeed able to demonstrate selective heteromeric self-sorting (Figure 2c), after initially forming a statistical mixture on the first assembly level. Ligand **B3** has a ribbon-shaped 3D structure and assembles into a $Pd_2(\mathbf{B3})_4$ capsule when mixed with Pd(II) in CD_3CN.[18] We previously reported that combining **B2** and **B3** in CD_3CN leads to the formation of a statistical mixture of cages in solution from which the crystal structure of the *trans*-$Pd_2(\mathbf{B2})_2(\mathbf{B3})_2$ cage was obtained.[27]

We now added homoleptic assembly $Pd_2\mathbf{A}_3(MeCN)_2$ to this mixture (in 8/3 ratio) and heated it at 70 °C for 24 h, after which we observed the emergence of two separate species, corresponding to the two co-existing heteroleptic cages $Pd_2\mathbf{A}_2(\mathbf{B2})_2$ and $Pd_2\mathbf{A}_2(\mathbf{B3})_2$ (Figures S9-15 and S37-41), as further confirmed by ESI-MS analysis and their separate syntheses. Each of these species contributes a single set of signals to ^{1}H-NMR spectrum of the mixture, similar to what was observed for $Pd_2\mathbf{A}_2(\mathbf{B1})_2$. The same self-sorting occurs when using **A**, **B1** and **B3** (Figures S42-43), with **B1** and **B2** being essentially isostructural.

Based on our knowledge of the crystal structure of $Pd_2\mathbf{A}_2(\mathbf{B1})_2$ and the aforementioned NMR analysis, it is safe to assume that the two obtained species possess a figure-of-eight topology with **B2** or **B3** sitting on the lateral faces of the respective assembly (Figure S54). Very interestingly here, the geometrical differences between **B2** and **B3** do not allow them to narcissistically or integratively sort in their binary mixture (so without **A**) and instead, their combination with Pd(II) cations leads to a statistical mixture of species. However, the differences are pronounced enough to further drive the heteromeric completive process once **A** is introduced. In this further degree of self-sorting, two discrete heteroleptic assemblies co-exist in a defined mixture without interfering. The component stoichiometry is a crucial parameter of the system as it allows the sole formation of the pair of heteroleptic assemblies. While showing pronounced structural flexibility,[27] ligand **B3** prefers to pair narcissistically with itself in $Pd_2\mathbf{A}_2(\mathbf{B3})_2$ (Pd-Pd distance = 15.0 Å) while **B2** then cleanly forms the more elongated $Pd_2\mathbf{A}_2(\mathbf{B2})_2$ structure (Pd-Pd distance = 15.6 Å). We assume that the energetic cost of bringing **B2** together with **B3**, requiring to either stretch **B3** to the length dictated by rigid **B2** or force the Pd coordination sites to tilt (under the constraint of the closely packed figure-of-eight situation) is higher than the tentative entropic gain of statistically scrambling **B2** and **B3** within the assemblies.

While here, heteromeric completive self-sorting could be induced by adding ligand **A** to a mixture of assemblies not capable of self-sorting on their own, we were curious to understand if this process can also emerge with components that are capable of undergoing a first degree of integrative sorting in their binary mixture.

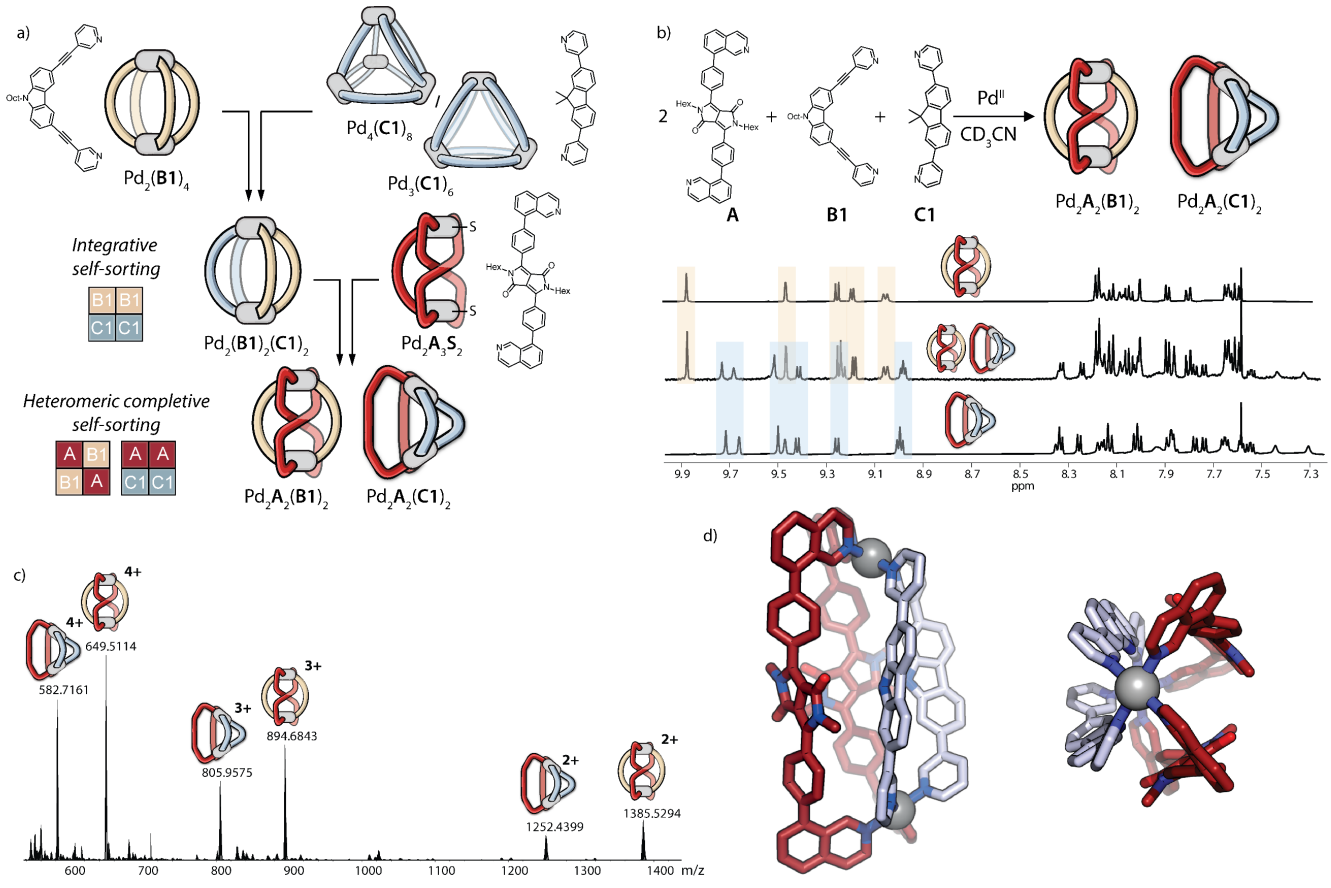

Figure 3. (a) Schematic representation of the step-by-step formation of heteromeric self-sorting where two heteroleptic assemblies co-exist in a 1:1 manner. (b) Stacked ^{1}H-NMR (CD_3CN, 500 MHz) spectra. From top to bottom: $Pd_2\mathbf{A}_2(\mathbf{B1})_2$ only, mixture $Pd_2\mathbf{A}_2(\mathbf{B1})_2$ and $Pd_2\mathbf{A}_2(\mathbf{C1})_2$, $Pd_2\mathbf{A}_2(\mathbf{C1})_2$ only. S = solvent molecules, herein acetonitrile. (c) HR-ESI-MS of the mixture of $Pd_2\mathbf{A}_2(\mathbf{B1})_2$ and $Pd_2\mathbf{A}_2(\mathbf{C1})_2$. c) X-ray single crystal structure of cage $Pd_2\mathbf{A}_2(\mathbf{C2})_2$, showing a *cis*-arrangement of the ligands and the symmetry breaking due to ligand twist and steric hindrance. Hexyl chains on the backbone of **A** are omitted for clarity.

Dimethyl-fluorene-based ligand **C1** features a large binding angle and its homoleptic assembly with Pd(II) cations leads to a mixture of a Pd_4(**C1**)$_8$ tetrahedron and a Pd_3(**C1**)$_6$ ring.[43] When both **B1** and **C1** are combined in a 1:1:1 ratio with $[Pd(MeCN)_4](BF_4)_2$ in acetonitrile, heteroleptic cage Pd_2(**B1**)$_2$(**C1**)$_2$ emerges as sole product through integrative self-sorting. When combined in a 1:1:1 ratio with Pd(II) in CD_3CN, **A** and **C1** yield another heteroleptic assembly Pd_2**A**$_2$(**C1**)$_2$, as confirmed by HR-ESI mass spectrometry (Figures S16-23). Owing to the diverging binding vectors of the smaller ligand **C1**, we excluded the possibility of forming a *trans*-figure-of-eight assembly when combined with **A** (Figure S54). Therefore, we assume this assembly to show a *cis*-heteroleptic cage topology with ligands positioned by shape complementarity. According to our previous observations,[9] the formation of such a *cis*-cage should lead to a single set of signals for each ligand in the ^{1}H NMR spectrum as usually no further symmetry breaking would be expected. However, analysis of this cage by NMR spectroscopy reveals a two-fold splitting of all proton signals (Figure 3b). Further DOSY NMR confirmed that all signals belonged to a single unique assembly.

While we were not able to obtain crystals for heteroleptic cage Pd_2**A**$_2$(**C1**)$_2$, replacing ligand **C1** by carbazole analog **C2** allowed us to grow crystals suitable for X-ray diffraction analysis. The geometrical similarities, in terms of binding angles, between the two ligands led us to infer that they form the same type of *cis*-heteroleptic cage. This was further indicated by observing the same patterns in both ^{1}H-NMR and ESI-MS spectra (Figures S24-26). Indeed, the crystal structure of Pd_2**A**$_2$(**C2**)$_2$ revealed the expected *cis*-$Pd_2A_2B_2$ arrangement (Figure 3d). The crystal structure further allows us to explain the two-fold splitting observed in the proton NMR spectra of both Pd_2**A**$_2$(**C1**)$_2$ and Pd_2**A**$_2$(**C2**)$_2$. Unlike the situation observed in other *cis*-heteroleptic cages, e.g. Pd_2(**B1**)$_2$(**C1**)$_2$, featuring only one NMR signal set, the buckled shape of ligand **A** caused by the diketopyrrolopyrrole moieties, leads to a symmetry breaking in the overall system. Inspection of the X-ray structure further indicates that rotation of the cores of ligand **A** is not possible due to the four hexyl chains hindering motion within the assembly. VT-NMR analysis (Figure S22) showed that even increasing the temperature to 90 °C in DMSO did not lead to a merging of the two ^{1}H-NMR signal sets, showing that rotation of the backbones is even hindered at elevated temperatures.

Next, we aimed at further increasing complexity and therefore mixed **A**, **B1** and **C1** with $[Pd(MeCN)_4](BF_4)_2$ in a 2:1:1:2 ratio in CD_3CN (Figure 3a). After 24 hours of heating at 70 °C, the ^{1}H-NMR spectrum of the equilibrated mixture depicts a perfect overlap of the two separate heteroleptic assemblies Pd_2**A**$_2$(**B1**)$_2$ and Pd_2**A**$_2$(**C1**)$_2$ (Figure 3b). Prolonged heating over one week did not alter the outcome of the reaction, letting us infer that this represents the thermodynamic state of the system. Analysis by ESI-MS also confirmed the clean formation of both heteroleptic species in the mixture (Figure 3c), showing prominent peaks for the $[Pd_2$**A**$_2$(**C1**)$_2]^{4+}$ and $[Pd_2$**A**$_2$(**C1**)$_2]^{4+}$ species as well as corresponding 3+ and 2+ charged assemblies with one and two associated BF_4^- counter anions, respectively (Figures S50-53).

To further show that this represents the thermodynamic minimum of the system, we performed a sequence of two cage-to-cage transformations (Figures S45-46). A mixture of homoleptic cages Pd_2(**B1**)$_4$ and Pd_3(**C1**)$_6$/Pd_4(**C1**)$_8$ was heated at 70 °C degrees for 12 hours to afford heteroleptic cage Pd_2(**B1**)$_2$(**C1**)$_2$ This assembly was further mixed with the homoleptic species Pd_2**A**$_3$(MeCN)$_2$ at 70 °C and yielded the same 1:1 mixture of Pd_2**A**$_2$(**B1**)$_2$ and Pd_2**A**$_2$(**C1**)$_2$. Interestingly, the sequential cage-to-cage transformation also demonstrates the favorable formation of the pair Pd_2**A**$_2$(**B1**)$_2$ and Pd_2**A**$_2$(**C1**)$_2$ over assembly Pd_2(**B1**)$_2$(**C1**)$_2$, with ligands exchanging between the cages. In a similar manner, the three homoleptic species can be mixed to obtain the final pair of co-existing heteroleptic structures. In this example, all components can form homoleptic assemblies as well as discrete $Pd_2A_2B_2$-type heteroleptic structures in opposition to the aforementioned cases. The importance of stoichiometry was further corroborated by control experiments in which the relative ratio of **A**, **B1,** and **C1** was varied for the self-assembly process (Figure S48). No precise self-sorting is observed when the stoichiometry differs from the aforementioned.

The versatility of ligand **A** should also be highlighted here. In the co-existing assemblies Pd_2**A**$_2$(**B1**)$_2$ and Pd_2**A**$_2$(**C1**)$_2$, it adopts two different conformations (*transoid*, S shape and *cisoid*, C shape) and pairwise arrangements (*trans* and *cis*), allowing the formation of both a *trans*-configured self-penetrated assembly and a non-entangled *cis*-cage (Figure S55).

Being able to dictate the population of species, arising from the use of three different ligands, was then our next interest in order to gain an even higher level of control over the system. The possibility to switch between different types of self-sorting within the same system upon application of a stimulus would potentially allow the regulation of various intra- and/or intermolecular functions involving these self-assembled hosts in a systems chemistry setting (Figure 4).

Indeed, when using mixtures of **A**, **B3** and **C1** we realized that it is possible to swing between either strict integrative or heteromeric completive self-sorting by varying the stoichiometry. We demonstrate this for switching between a mixture of Pd_2**A**$_2$(**B3**)$_2$/Pd_2**A**$_2$(**C1**)$_2$ and *trans*-cage Pd_2**A**(**B3**)$_2$(**C1**).

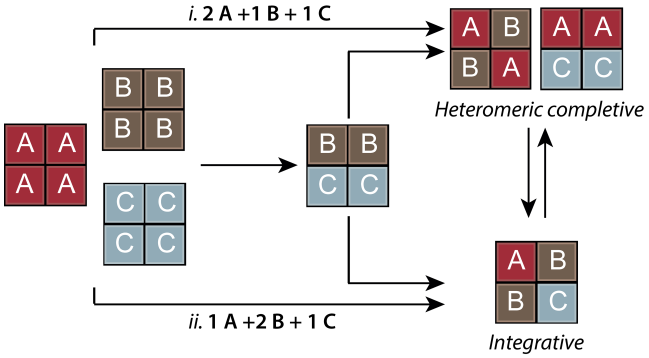

Figure 4. Heteromeric completive or integrative self-sorting can be controlled through variation of component ratios in a three ligands system. This allows to switch between two discrete co-existing binary heteroleptic cages and a single, structurally more complex ternary assembly.

The combination of ligands **B3** and **C1** was previously reported to undergo integrative self-sorting and form a Pd_2(**B3**)$_2$(**C1**)$_2$ *cis*-heteroleptic cage.[27] The subsequent addition of the homoleptic assembly of **A** leads again to heteromeric completive self-sorting, and the co-existence of the two heteroleptic species was confirmed by ^{1}H NMR and ESI-MS (Figure 5a). We were able to grow red needle-shaped crystals suitable for X-ray analysis. The obtained crystal structure was not the expected one but was found to be the *trans*-Pd_2**A**(**B3**)$_2$(**C1**) architecture (Figure 5d).

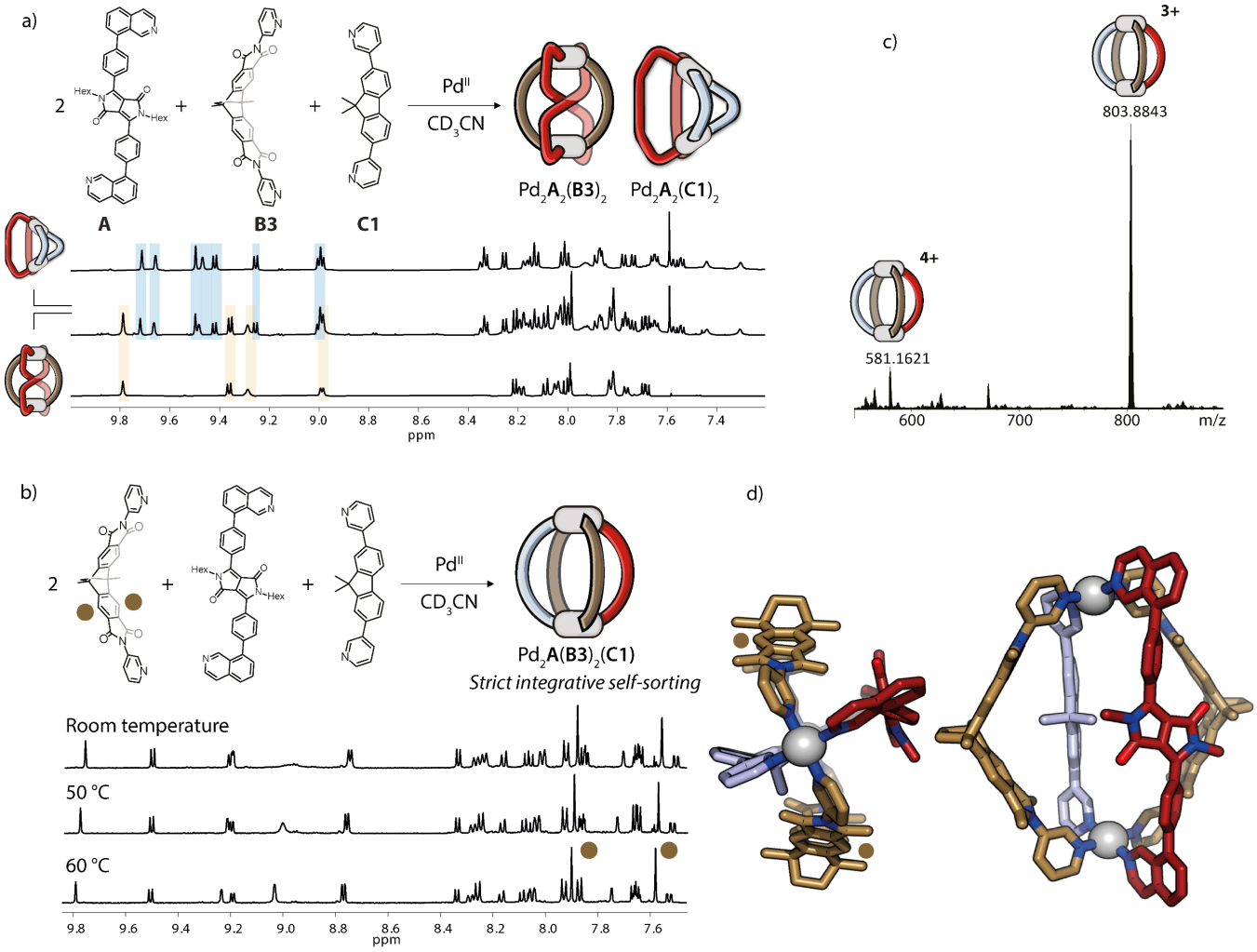

Figure 5. (a) Heteromeric completive self-sorting is achieved when **A**, **B3** and **C1** are mixed together in a 2:1:1 ratio with Pd(II). The stack of 1H-NMR spectra (CD_3CN, 500 MHz) shows a perfect overlap of the two separate species. (b) Strict integrative self-sorting of **A**, **B3** and **C1** when combined in a 1:1:2 ratio. The ^1H NMR (CD_3CN, 500 MHz) shows protons sharpening. The two non-equivalent proton positions of **B3** are highlighted with brown dots. (c) HR-ESI-MS of Pd_2**A**(**B3**)$_2$(**C1**) showing prominent peaks for the species with a 4+ charge as well as 3+ charge with associated counter anions, (d) X-ray crystal structure of Pd_2**A**(**B3**)$_2$(**C1**) with a *trans*-configuration. The two non-equivalent proton positions of **B3** are highlighted with brown dots.

In this structure, **A** and **C1** present shape complementarity vectors and assemble together in a *trans*-configuration while two more flexible ligands **B3** sit face-to-face to each other completing the coordination sphere of the Pd(II) centers. Herein, ligand **A** is adopting a third structural motif within this study, sitting as a single unit in its *cisoid* form opposite to ligand **C1**. We further show that mixing the ligands in the appropriate ratio yields this *trans*-Pd_2**A**(**B3**)$_2$(**C1**) assembly (Figures S27-34), selectively (Figure 5b). This proves that the newly formed cage is not only a product of the crystallization process and can be isolated as a sole species in solution, in contrast to above discussed Pd_2(**B1**)A_2(**B2**). Every ligand leads to one set of signals in the ^1H-NMR spectrum of Pd_2**A**(**B3**)$_2$(**C1**). While the signals of the pyridyl protons of **B3** are rather broad at RT, VT-NMR allows their sharpening when a temperature of 60 °C is reached. The lateral protons H of **B3** (marked as brown dots), however, split into two sets as highlighted in Figure. 5b, as the left- and right-sided protons are facing a distinct neighboring ligand, i.*e.* **A** or **C1**, making them chemically non-equivalent. ESI-MS analysis further confirmed the formation of a single assembly with prominent peaks observable for the species with a 4+ charge as well as 3+ charge with associated counter anions (Figure. 5c).

This triad of ligands therefore allows a finer tuning of the self-sorting by variation of the ratio of components. We were further able to reversibly switch between heteromeric completive and integrative self-sorting by addition of suitable amounts of ligands and Pd(II) cations, respectively, to preformed species (two cycles were performed and can be found in Figure S53). This stoichiometry control thus allows the increase in complexity to either yield a single ternary assembly or a pair of co-existing binary cages

Conclusion

We herein report the first example of heteromeric completive self-sorting in coordination cage systems. Two heteroleptic assemblies based on three different ligands (A, B and C) can co-exist in a discrete fashion without undergoing a shuffling of their components. This behavior can emerge into two different scenarios. On the one hand, when components B and C lead to a statistical mixture of assemblies, the introduction of

component A leads to the clean formation and co-existence of binary systems $Pd_2A_2B_2$ and $Pd_2A_2C_2$. On the other hand, we also showed that if other derivatives of B and C can first yield a defined $Pd_2B_2C_2$ assembly through integrative self-sorting, addition of A can again lead to the same result of heteromeric completive self-sorting. This paves the way for the creation of dynamic populations of coordination cages and control of their composition (and associated function) upon application of a stimulus. We here show that subtle variation of the kind and stoichiometry of component controls the sorting of the system. Both, architectures with similar or different topologies, namely a *cis*-cage or a figure-of-eight *trans*-ravel, can co-exist, offering possibilities for tuning the structure of the discrete species, hence offering potential for implementing different functionalities. Finally, we demonstrate control over heteromeric vs. integrative self-sorting by adjusting the ligand ratio, thereby switching from a cage population comprising two binary structures to a sole discrete ternary assembly. We are currently exploiting this responsiveness, combined with photo-switchable components,[44] to develop complex systems showing emergence of intra- or intermolecular functionality, e.g. in the form of adjustable catalytic activity or information processing features.

ASSOCIATED CONTENT

Synthetic procedures, NMR, MS, SCXRD results and calculation data are included in the Supporting Information. CCDC numbers: 2310126, 2310127 and 2310128 contain the crystallographic data. This material is available free of charge via the Internet at http://pubs.acs.org.

AUTHOR INFORMATION

Corresponding Author

*guido.clever@tu-dortmund.de

ORCID

Irene Regeni: 0000-0001-9102-3053
Elie Benchimol: 0000-0001-5741-7075
Julian J. Holstein: 0000-0002-8385-7805
Guido H. Clever: 0000-0001-8458-3060

Author Contributions

All authors have given approval to the final version of the manuscript. ‡These authors contributed equally.

Notes

The authors declare no competing financial interests.

ACKNOWLEDGMENT

This work was supported by the Deutsche Forschungsgemeinschaft (DFG) trough GRK2376 ("Confinement-Controlled Chemistry", project number 331085229) and under Germany's Excellence Strategy EXC2033, project number 390677874 ("RESOLV"). I.R. thanks the Fonds der Chemischen Industrie (FCI) for a Kekulé PhD fellowship. Diffraction data of $[Pd_2\mathbf{A}_2(\mathbf{C1})_2]$, $[Pd_2\mathbf{A}_1(\mathbf{B3})_2(\mathbf{C1})_1]$ and $[Pd_2\mathbf{A}_2(\mathbf{B1})_1(\mathbf{B2})_1]$ was collected at PETRA III and processed on the Maxwell computational resources operated at DESY (Hamburg, Germany) a member of the Helmholtz Association (HGF). We thank Guillaume Pompidor, Helena Taberman and Eva Crosas for assistance at synchrotron beamline P11 (STP-20010393, I-20211437, I-2021092) and DESY user office for travel funds.

REFERENCES

(1) Lehn, J. Perspectives in Supramolecular Chemistry—From Molecular Recognition towards Molecular Information Processing and Self-Organization. *Angew. Chem. Int. Ed.* **1990**, *29*, 1304–1319.

(2) Lehn, J.-M. From Supramolecular Chemistry towards Constitutional Dynamic Chemistry and Adaptive Chemistry. *Chem. Soc. Rev.* **2007**, *36*, 151-160.

(3) Safont-Sempere, M. M.; Fernández, G.; Würthner, F. Self-Sorting Phenomena in Complex Supramolecular Systems. *Chem. Rev.* **2011**, *111*, 5784–5814.

(4) He, Z.; Jiang, W.; Schalley, C. A. Integrative Self-Sorting: A Versatile Strategy for the Construction of Complex Supramolecular Architecture. *Chem. Soc. Rev.* **2014**, *44*, 779–789.

(5) Mukhopadhyay, P.; Wu, A.; Isaacs, L. Social Self-Sorting in Aqueous Solution. *J. Org. Chem.* **2004**, *69*, 6157–6164.

(6) Jiang, W.; Wang, Q.; Linder, I.; Klautzsch, F.; Schalley, C. A. Self-Sorting of Water-Soluble Cucurbituril Pseudorotaxanes. *Chem. Eur. J.* **2011**, *17*, 2344–2348.

(7) Wu, A.; Isaacs, L. Self-Sorting: The Exception or the Rule? *J. Am. Chem. Soc.* **2003**, *125*, 4831–4835.

(8) Jiang, W.; Schalley, C. A. Integrative Self-Sorting Is a Programming Language for High Level Self-Assembly. *Proc. Natl. Acad. Sci.* **2009**, *106*, 10425–10429.

(9) Pullen, S.; Tessarolo, J.; Clever, G. H. Increasing Structural and Functional Complexity in Self-Assembled Coordination Cages. *Chem. Sci.* **2021**, *12*, 7269–7293.

(10) Li, J.-R.; Zhou, H.-C. Bridging-Ligand-Substitution Strategy for the Preparation of Metal–Organic Polyhedra. *Nat. Chem.* **2010**, *2*, 893-898.

(11) Sun, Q.; Sato, S.; Fujita, M. An $M_{12}(L1)_{12}(L2)_{12}$ Cantellated Tetrahedron: A Case Study on Mixed-Ligand Self-Assembly. *Angew. Chem. Int. Ed.* **2014**, *53*, 13510–13513.

(12) Sudan, S.; Li, R.-J.; Jansze, S. M.; Platzek, A.; Rudolf, R.; Clever, G. H.; Fadaei-Tirani, F.; Scopelliti, R.; Severin, K. Identification of a Heteroleptic $Pd_6L_6L'_6$ Coordination Cage by Screening of a Virtual Combinatorial Library. *J. Am. Chem. Soc.* **2021**, 143, 1773–1778.

(13) Platzek, A.; Juber, S.; Yurtseven, C.; Hasegawa, S.; Schneider, L.; Drechsler, C.; Ebbert, K. E.; Rudolf, R.; Yan, Q.; Holstein, J. J.; Schäfer, L. V.; Clever, G. H. Endohedrally Functionalized Heteroleptic Coordination Cages for Phosphate Ester Binding. *Angew. Chem. Int. Ed.* **2022**, *61*, e202209305.

(14) Findlay, J. A.; Patil, K. M.; Gardiner, M. G.; MacDermott-Opeskin, H. I.; O'Mara, M. L.; Kruger, P. E.; Preston, D. Heteroleptic Tripalladium(II) Cages. *Chem. Asian. J.* **2022**, *17*, e202200093.

(15) Li, S.-C.; Cai, L.-X.; Hong, M.; Chen, Q.; Sun, Q.-F. Combinatorial Self-Assembly of Coordination Cages with Systematically Fine-Tuned Cavities for Efficient Co-Encapsulation and Catalysis. *Angew. Chem. Int. Ed.* **2022**, *61*, e2022047.

(16) Xuan, J.-J.; Xia, Z.-J.; Yan, D.-N.; Hu, S.-J.; Zhou, L.-P.; Cai, L.-X.; Sun, Q.-F. Shape Complementary Coordination Self-Assembly of a Redox-Active Heteroleptic Complex. *Inorg. Chem.* **2022**, *61*, 8854–8860.

(17) Chen, B.; Holstein, J. J.; Platzek, A.; Schneider, L.; Wu, K.; Clever, G. H. Cooperativity of Steric Bulk and H-Bonding in Coordination Sphere Engineering: Heteroleptic Pd^{II} Cages and Bowls by Design. *Chem. Sci.* **2022**, *13*, 1829–1834.

(18) Chen, B.; Holstein, J. J.; Horiuchi, S.; Hiller, W. G.; Clever, G. H. Pd(II) Coordination Sphere Engineering: Pyridine Cages, Quinoline Bowls, and Heteroleptic Pills Binding One or Two Fullerenes. *J. Am. Chem. Soc.* **2019**, *141*, 8907–8913.

(19) Lewis, J. E. M. Pseudo-heterolepticity in Low-Symmetry Metal-Organic Cages. *Angew. Chem. Int. Ed.* **2022**, *61*, e202212392.

(20) Yoshizawa, M.; Nakagawa, J.; Kumazawa, K.; Nagao, M.; Kawano, M.; Ozeki, T.; Fujita, M. Discrete Stacking of Large Aromatic Molecules within Organic-Pillared Coordination Cages. *Angew. Chem. Int. Ed*. **2005**, *44*, 1810–1813.

(21) Preston, D.; Barnsley, J. E.; Gordon, K. C.; Crowley, J. D. Controlled Formation of Heteroleptic $[Pd2(La)_2(Lb)_2]^{(4+)}$ Cages. *J. Am. Chem. Soc.* **2016**, *138*, 10578–10585.

(22) Holloway, L. R.; Bogie, P. M.; Hooley, R. J. Controlled Self-Sorting in Self-Assembled Cage Complexes. *Dalton. Trans.* **2017**, *46*, 14719–14723.

(23) Rizzuto, F. J.; Carpenter, J. P.; Nitschke, J. R. Multi-Site Binding of Drugs and Natural Products in an Entropically-Favorable, Heteroleptic Receptor. *J. Am. Chem. Soc.* **2019**, *141*, 9087–9095.

(24) Ronson, T. K.; Carpenter, J. P.; Nitschke, J. R. Dynamic Optimization of Guest Binding in a Library of Diastereomeric Heteroleptic Coordination Cages. *Chem* **2022**, *8*, 557–568.

(25) Yamashina, M.; Yuki, T.; Sei, Y.; Akita, M.; Yoshizawa, M. Anisotropic Expansion of an M2L4 Coordination Capsule: Host Capability and Frame Rearrangement. *Chem. Eur. J.* **2015**, *21*, 4200–4204.

(26) Yang, Y.; Ronson, T. K.; Hou, D.; Zheng, J.; Jahović, I.; Luo, K. H.; Nitschke, J. R. Hetero-Diels–Alder Reaction between Singlet Oxygen and Anthracene Drives Integrative Cage Self-Sorting. *J. Am. Chem. Soc.* **2023**, *145*, 19164–19170.

(27) Wu, K.; Benchimol, E.; Baksi, A.; Clever, G. Non-statistical assembly of Multicomponent [Pd_2ABCD] Cages. *Nat. Chem.* **2024**, DOI: 10.1038/s41557-023-01415-7.

(28) Li, R.-J.; Montmollin, J. de; Fadaei-Tirani, F.; Scopelliti, R.; Severin, K. Construction of Pd-Based Coordination Cages with Three Geometrically Distinct Ligands. *Dalton Trans.* **2023**, *52*, 6451–6456.

(29) Liu, Y.; Liao, S.; Dai, W.; Bai, Q.; Lu, S.; Wang, H.; Li, X.; Zhang, Z.; Wang, P.; Lu, W.; Zhang, Q. Controlled Construction of Heteroleptic $[Pd_2(LA)_2(LB)(LC)]^{4+}$ Cages: A Facile Approach for Site-Selective Endo-Functionalization of Supramolecular Cavities. *Angew. Chem. Int. Ed.* **2023**, *62*, e202217215.

(30) Abe, T.; Sanada, N.; Takeuchi, K.; Okazawa, A.; Hiraoka, S. Assembly of Six Types of Heteroleptic Pd2L4 Cages under Kinetic Control. *J. Am. Chem. Soc.* **2023**, *51*, 28061–28074.

(31) Preston, D.; Evans, J. D. A Lantern-Shaped Pd(II) Cage Constructed from Four Different Low-Symmetry Ligands with Positional and Orientational Control: An Ancillary Pairings Approach. *Angew. Chem. Int. Ed.* **2023**, *62*, e202314378.

(32) Zheng, Y.; Yang, H.; Ghosh, K.; Zhao, L.; Stang, P. J. Multicomponent Supramolecular Systems: Self-Organization in Coordination-Driven Self-Assembly. *Chem. Eur. J.* **2009**, *15*, 7203–7214.

(33) Zhao, J.; Xing, P. Regulation of Circularly Polarized Luminescence in Multicomponent Supramolecular Coassemblies. *ChemPhotoChem* **2022**, *6,* e20210012.

(34) Matsuno, T.; Sato, S.; Yokoyama, A.; Kamata, S.; Isobe, H. Self-Sorting of Two Hydrocarbon Receptors with One Carbonaceous Ligand. *Angew. Chem. Int. Ed.* **2016**, *128*, 15565–15569.

(35) Yang, Z.; Esteve, F.; Antheaume, C.; Lehn, J.-M. Dynamic Covalent Self-Assembly and Self-Sorting Processes in the Formation of Imine-Based Macrocycles and Macrobicyclic Cages. *Chem. Sci.* **2023**, *14*, 6631–6642.

(36) Gu, R.; Lehn, J.-M. Constitutional Dynamic Selection at Low Reynolds Number in a Triple Dynamic System: Covalent Dynamic Adaptation Driven by Double Supramolecular Self-Assembly. *J. Am. Chem. Soc.* **2021**, *143*, 14136–14146.

(37) Esteve, F.; Altava, B.; García-Verdugo, E.; Luis, S. V.; Lehn, J.-M. Doubly Chiral Pseudopeptidic Macrobicyclic Molecular Cages: Water-Assisted Dynamic Covalent Self-Assembly and Chiral Self-Sorting. *Chem* **2022**, *8*, 2023-2042.

(38) Regeni, I.; Chowdhury, R.; Terlinden, K.; Horiuchi, S.; Holstein, J. J.; Feldmann, S.; Clever, G. H. Engineering Soluble Diketopyrrolopyrrole Chromophore Stacks from a Series of Pd(II)-Based Ravels. *Angew. Chem. Int. Ed.* **2023**, *62*, e202308288.

(39) Saha, M. L.; Schmittel, M. Degree of Molecular Self-Sorting in Multicomponent Systems. *Org. Biomol. Chem.* **2012**, *10*, 4651–4684.

(40) Benchimol, E.; Nguyen, B.-N. T.; Ronson, T. K.; Nitschke, J. R. Transformation Networks of Metal–Organic Cages Controlled by Chemical Stimuli. *Chem. Soc. Rev.* **2022**, *51*, 5101–5135.

(41) Zhu, R.; Lübben, J.; Dittrich, B.; Clever, G. H. Stepwise Halide-Triggered Double and Triple Catenation of Self-Assembled Coordination Cages. *Angew. Chem. Int. Ed.* **2015**, *54*, 2796–2800.

(42) Ebbert, K. E.; Schneider, L.; Platzek, A.; Drechsler, C.; Chen, B.; Rudolf, R.; Clever, G. H. Resolution of Minor Size Differences in a Family of Heteroleptic Coordination Cages by Trapped Ion Mobility ESI-MS. *Dalton Trans.* **2019**, *48*, 11070-11075.

(43) Wu, K.; Zhang, B.; Drechsler, C.; Holstein, J. J.; Clever, G. H. Backbone-Bridging Promotes Diversity in Heteroleptic Cages. *Angew. Chem. Int. Ed.* **2020**, *60*, 6403–6407.

(44) Benchimol, E.; Tessarolo, J.; Clever, G. H. Photoswitchable Coordination Cages. *Nat. Chem.* **2024**, *16*, 13–21.

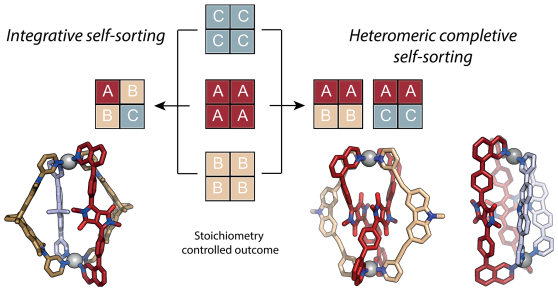
Integrative self-sorting
Heteromeric completive self-sorting
Stoichiometry controlled outcome